processes

MDPI

Article

Tandem-Homodimer of a β-Sheet-Forming Short Peptide Inhibits Random-to-β Structural Transition of Its Original Monomer

Kin-ya Tomizaki [1,2,*], Tomomi Iori [1], Hideyasu Fukushima [1], Yasuhiro Nakabayashi [1], Yoshiki Matsumoto [1] and Takahito Imai [1]

[1] Department of Materials Chemistry, Ryukoku University, Seta-Oe, Otsu 520-2194, Japan; sgnav038y@gmail.com (T.I.); hi.fukushima@outlook.jp (H.F.); 0605nakaba@gmail.com (Y.N.); matsu_yoshi9273@yahoo.co.jp (Y.M.); imai@rins.ryukoku.ac.jp (T.I.)

[2] Innovative Materials and Processing Research Center, Ryukoku University, Seta-Oe, Otsu 520-2194, Japan

* Correspondence: tomizaki@rins.ryukoku.ac.jp; Tel.: +81-77-543-7469; Fax: +81-77-453-7483

Received: 18 October 2020; Accepted: 6 November 2020; Published: 8 November 2020

Abstract: There is an increasing interest in designing fibrillogenesis modulators for treating amyloid β (Aβ)-peptide-associated diseases. The use of Aβ fragment peptides and their derivatives, as well as nonpeptidyl natural products, is one promising approach to prevent Aβ fibrillation. In this study, we demonstrate that tandem-homodimers (TDs) of a β-sheet-forming short peptide in which the amino acid sequence is duplicated in series and joined via an amino alkanoic acid linker of different chain lengths, preventing the random-to-β structural transition of the original monomer. Ape5-TD, containing 5-amino pentanoate, most potently prevented this transition for at least five days by generating disordered aggregates with reduced tryptic stability. The linkers in the TDs generated this inhibitory activity, probably due to their bent conformations and hydrophobicity, appropriate for accommodating and twisting the monomers, resulting in irregular arrangements of the peptides. The present study could allow the design of a new class of protein/peptide fibrillogenesis modulators.

Keywords: peptide; self-assembly; fibrillation; inhibitor; modulator; amyloid β peptide

1. Introduction

Amyloid fibrils, generated by the progression of protein misfolding and aggregation, are closely associated with several severe amyloid diseases such as Alzheimer's, Parkinson's, and Creutzfeldt–Jakob [1]. Senile amyloid plaques are observed in brain tissue from Alzheimer's disease (AD) patients and consist primarily of aggregated amyloid β (Aβ) peptides, 40 and 42 amino acid residues long. The aggregated amyloids contain characteristic cross-β-sheet fibrous structures with the β-strands orthogonal to the fibril axis [2]. Much effort has been devoted to uncovering the processes of Aβ peptide self-assembly and the progression of AD, resulting in the suggestion that the association of Aβ peptide monomers with neurotoxic oligomers triggers a pathologic cascade for AD development [3–6].

In general, protein fibrillation involves multiple self-assembling formations, including oligomers, protofibrils, and fibrils [7]. One of the most popular approaches to inhibiting toxic Aβ peptide self-assemblies, directing Aβ fibrils, has been the use of Aβ fragment peptides derived from the central hydrophobic cluster Aβ(17–21) and their related compounds, called β-sheet breakers [8–10]. Such Aβ fragment peptides may bind to the full-length Aβ peptide and inhibit subsequent elongation of Aβ fibrous arrangements. Additionally, nonpeptidyl small molecules [11–14] and polymeric macromolecules have been developed to modulate Aβ self-assembly, facilitating fibril formation and inhibiting Aβ peptide association processes [15,16].

Intermediate oligomeric aggregates produced during Aβ peptide fibrillation have recently gathered attention because their cytotoxicity is higher than that of fibrous aggregates observed in senile amyloid plaques [17–22]. This has led to an alternative approach, employing peptides derived from the C-terminal region of the Aβ peptide to disrupt Aβ oligomer formation. The rationale behind this approach is that the Aβ(29–42) cluster of hydrophobic amino acids likely forms the hydrophobic cores of the oligomers [23–26]. Furthermore, Aβ peptide self-assembly can be modulated using other approaches, including Aβ peptides, in which two amino acids forming the turn region are replaced with β-turn mimetic linkers [27], a tandem peptide consisting of two Aβ peptides in which the retro sequence of the original Aβ peptide (Aβ40–1)) is joined with the original Aβ(1–40) via an eight glycine linker [28] and a 12-mer all-D-enantiomeric peptide, obtained using a mirror image phage display technique, and the resulting head-to-tail tandem peptide [29].

Promising methodologies to reduce the risk of AD pathogenesis and progression would include the development of modulators to inhibit Aβ peptide fibrillation or (preferably "and") eliminate highly toxic Aβ oligomers. These approaches would be beneficial if subsequent Aβ peptides, formed after modulation of Aβ-associating events, were proteolytically labile, allowing toxic species to be cleared from patients. This requires modulators that meet the following criteria: (i) binding to Aβ peptide at the early random coil structure stage [30], (ii) inhibiting the random-to-β structural transition of Aβ, and (iii) generating nonfibrous structures with reduced proteolytic stability for elimination [31].

We previously designed and synthesized the β-sheet-forming nonapeptide RU003 (Ac-AIEKAXEIA-NH_2, X = L-2-naphthylalanine, Nal) [32] and RU003 tandem-homodimers (TDs) in which the amino acid sequence of RU003 is duplicated and connected by amino alkanoic acid linkers with different chain lengths in a head-to-tail fashion and then characterized their self-assembled nanostructures [33]. We found that (i) the original RU003 sequence showed a random-to-β structural transition in water, (ii) RU003 tandem-homodimers, with a linker comprising 4-aminobutylic acid (Abu4), 5-amino pentanoic acid (Ape5), 6-amino hexanoic acid (Ahx6), 7-amino heptanoic acid (Ahp7), or 8-amino octanoic acid (Aoc8), formed β-sheet structures after five minutes' incubation, and (iii) RU003 TDs, with linkers comprising Abu4, Ape5, Ahx6 or Ahp7, showed significant diffraction peaks, likely corresponding to the molecular length of the hairpin (bent) conformations [33]. We assumed that if simple tandem-homodimerization of a β-sheet-forming peptide inhibited the random-to-β structural transition of the original peptide, the findings will aid the rational design of potent protein/peptide fibrillation inhibitors. Recently, L-2-naphthylalanine was also employed to improve the self-association propensity of gadolinium-complex-conjugated phenylalaninyl–phenylalanine (Phe–Phe) by replacing the Phe–Phe sequence with the Nal–Nal sequence [34]. Therefore, the use of Nal-containing peptides could be helpful as an Ab model system. In this study, we report the results of (i) kinetic experiments on the inhibition of the RU003 structural transition by adding RU003 TDs with linkers comprising Abu4 (Abu4-TD), Ape5 (Ape5-TD), Ahx6 (Ahx6-TD), Ahp7(Ahp7-TD), or Aoc8 (Aoc8-TD) during self-assembly, and (ii) morphological characterization and (iii) proteolytic stability of the subsequent self-assembled peptide nanostructures (Figure 1).

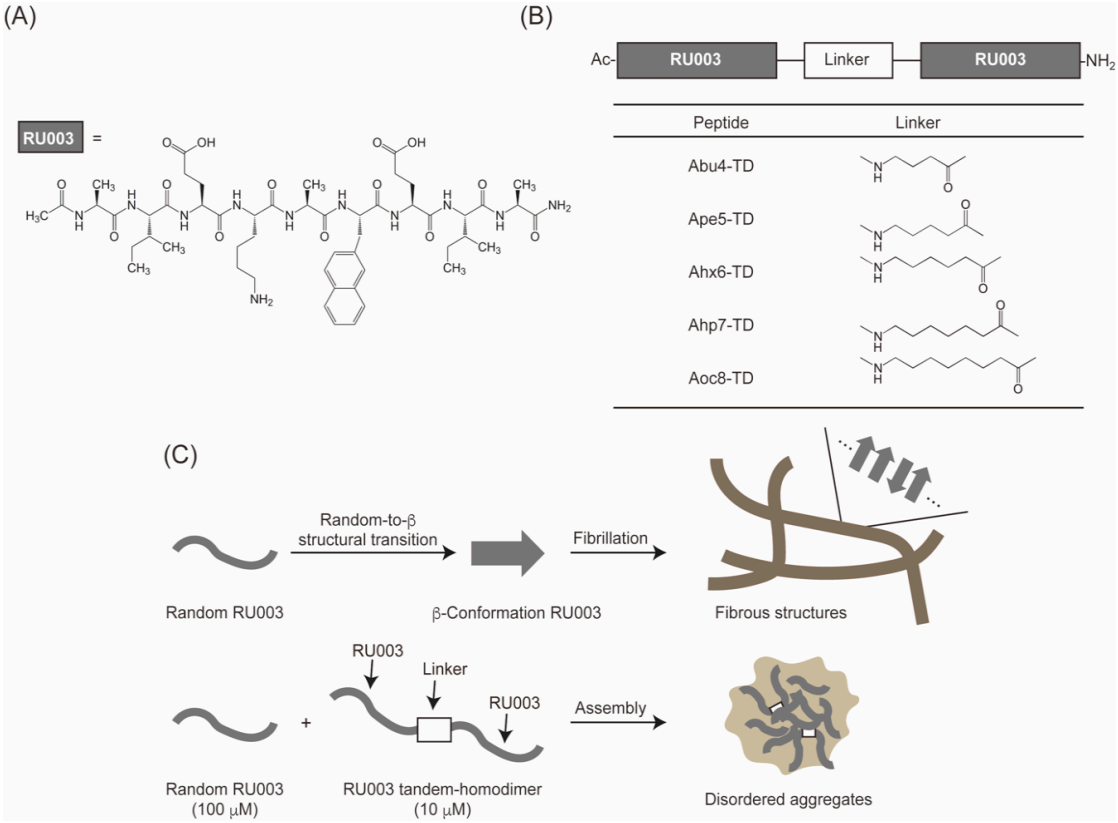

Figure 1. Amino acid sequences of the β-sheet-forming peptides. (**A**) The original nonapeptide RU003, (**B**) RU003 tandem-homodimers connected by an alkanoic amino acid with different chain lengths, and (**C**) inhibition of the random-to-β structural transition and subsequent fibrillation of RU003 by the tandem-homodimers.

2. Materials and Methods

2.1. General

Solvents and reagents were purchased from Wako Pure Chemical Industries (Osaka, Japan). Fmoc-amino acid derivatives and coupling reagents for peptide synthesis were purchased from Watanabe Chemical Industries (Hiroshima, Japan). Acetonitrile (high-perfoemance liquid chromatograpy (HPLC) grade) was purchased from Nacalai Tesque Inc. (Kyoto, Japan) and used for HPLC analysis and purification of peptides. All solvents and reagents were used as received.

2.2. Noncommercial Compounds

RU003, Abu4-TD, Ape5-TD, Ahx6-TD, Ahp7-TD, and Aoc8-TD were prepared according to the literature [32,33]. Characterization data (HPLC and matrix-assisted laser desorption/ionization time-of-flight mass spectrometry (MALDI–TOFMS)) are shown in Figures S1–S12).

2.3. Sample Preparation

Peptide stock solutions were prepared by dissolving each lyophilized powder in 1,1,1,3,3,3′-hexafluoro-2-propamol (HFIP) to prevent self-assembly during storage. The concentration of the RU003 stock solution was determined using an extinction coefficient of 5500 M^{-1} cm^{-1} for the Nal nonapeptide [35] in an aqueous solution containing 1% TFE (*v*/*v*) on a JASCO J-820 spectropolarimeter (JASCO, Tokyo Japan) using a quartz cuvette with a 1-mm pathlength. The concentrations of the stock solutions for RU003 tandem-homodimers were determined in the same manner as for RU003, using an extinction coefficient of 11,000 M^{-1} cm^{-1} for the two Nal residues in each sequence. The peptide stock

solutions were transferred to a microtube, mixed well, dried with a N_2 gas stream (Kyoto Teisan Inc., Kyoto, Japan), then dried in vacuo for 1 h. Ultrapure water (hereafter "water"; Wako Pure Chemical Industries, Osaka, Japan) was added to the microtube, and the mixture was stored at 40 °C for 15 min, then sonicated (Kaijo Sono Cleaner CA-44800, Tokyo, Japan) at 40 °C for 2 min to break up peptide aggregates. The obtained solution was incubated in a dry block heater (EB-303, As One, Osaka, Japan) at 40 °C for up to 5 days for maturation.

2.4. Circular Dichroism (CD) spectroscopy

CD spectra of the RU003 aqueous solutions ([RU003] = 100 μM) containing the RU003 tandem-homodimers ([RU003 TD] = 0, 5, 10, and 20 μM) at 0, 1, 2, 3, 4, and 5 day(s) after the start of incubation were acquired on a JASCO J-820 spectropolarimeter using a quartz cuvette with a 1-mm pathlength. An incubation period of "0 days" means "5 min after the reaction started".

2.5. Transmission Electron Microscopy (TEM)

Droplets of a solution containing the peptide were applied to a TEM grid (Cu 200 mesh covered with a collodion membrane; Nisshin EM, Tokyo, Japan) for 1 min and dried with filter paper. The sample was negatively stained with 2% phosphotungstic acid for 1 min, washed with water, and dried with filter paper. All TEM samples were dried in vacuo before conducting TEM measurements at an accelerating voltage of 200 kV (JEOL JEM-2100, Tokyo, Japan).

2.6. Atomic Force Microscopy (AFM)

A silicon wafer (p-Si(100), Mitsubishi Materials Co., Tokyo, Japan) was cut into 1 × 1 cm pieces and subjected to ultrasonic cleaning in acetone for 5 min (twice), followed by photocleaning with an ultraviolet ozonizer (Kenix KUV-100, Kenix, Himeji, Japan) at room temperature for 10 min. Droplets of the peptide solution were applied to the silicon substrates for 1 min, washed with water, and dried with filter paper. All AFM samples were dried in vacuo before conducting AFM measurements (MFP-3D-SA-J, Asylum Technology, Oxford Instruments, Tokyo, Japan) with a cantilever (Olympus OMCL-AC240TS-C3, Olympus, Tokyo, Japan).

2.7. Proteolytic Degradation

Tryptic Digestion: The peptide solutions ([RU003] = 100 μM and [Ape5-TD] = 0 or 10 μM in water, 50 μL), matured at 40 °C for 5 days, were mixed with 0.50 M $NaHCO_3$ (5.0 μL) and trypsin solution ([trypsin] = 0 or 1.0 x 10^{-2} g L^{-1} in water, 1.1 μL; trypsin from bovine pancreas; Sigma-Aldrich, Tokyo, Japan); then, the obtained solutions (RU003/trypsin = 490/1, *w*/*w*) were incubated at 40 °C for 1 h. The reaction mixtures were analyzed on a Hitachi LaChrom Elite HPLC system (Tokyo, Japan) using Cosmosil 5C_{18}-AR-II packed columns (4.6 × 150 mm, Nacalai Tesque, Kyoto, Japan) with a linear gradient of acetonitrile/0.1% TFA from 25% to 60% for 30 min at a flow rate of 1.0 mL min^{-1}.

α-Chymotryptic Digestion: As described in *Tryptic Digestion*, the peptide solutions (50 μL) were mixed with $NaHCO_3$ (5.0 μL) and the chymotrypsin solution ([α -chymotrypsin] = 0 or 1.0 g L^{-1} in water, 5.4 μL; α-chymotrypsin from bovine pancreas; Sigma-Aldrich, Tokyo, Japan) was added to prepare the reaction mixtures (RU003/ α -chymotrypsin = 1/1, *w*/*w*), followed by HPLC analysis.

3. Results and Discussion

3.1. Design, Synthesis, and Characterization of the Peptides

The designs of the β-sheet-forming nonapeptide RU003 and RU003 tandem-homodimers have been described previously [32,33]. Briefly, RU003 comprises two L-isoleucines (Ile) at the 2nd and 8th positions and an aromatic L-2-naphthylalanine (Nal) at the 6th position. These hydrophobic amino acids provide the driving force for self-assembly into a β-sheet conformation via hydrophobic interactions and/or π–π stacking (Figure 1A). Two L-glutamic acids (Glu) are present at the 3rd and 7th

positions to make the peptide water-soluble and amphiphilic (binary pattern) in a β-sheet conformation. An L-lysine (Lys) is located at the 4th position on the hydrophobic side and neighboring the Nal residue to stabilize the β-sheet conformation via possible cation–π interaction between the aminium cation and the naphthalene side chain. The RU003 tandem-homodimers were designed by copying the RU003 sequence and joining two sequences together with an amino alkanoic acid linker of different chain lengths in a head-to-tail fashion (Figure. 1B). Peptides were prepared by standard solid-phase peptide synthesis using Fmoc chemistry [36], purified by reverse-phase HPLC, and characterized by MALDI–TOFMS (Figures S1–S12).

3.2. CD Measurements of RU003 Monomer and RU003 TDs alone

First, we analyzed the secondary structures of RU003 (100 μM) in the absence and presence of the five tandem-homodimers, with concentrations ranging from 5.0 to 20 μM by measuring CD spectra at incubation periods ranging from 0 (5 min after starting the reaction) to 5 days. Here, we show time-dependent CD spectra of RU003 (100 μM, Figure 2A) obtained at 1-day intervals. The CD spectra of RU003 exhibited a strong negative peak at 200 nm at both day-0 and day-1, corresponding to a random coil (disordered) structure [37,38]. A significant change was observed at day-2, with positive and negative peaks at 200 and 225 nm, respectively, corresponding to β-sheet structure, and these peaks were observed for the duration of the experiment (5 days). The CD spectrum of Ac-KEFFFFKE-NH_2 was recently reported to show positive and negative peaks at 205 and 230 nm, respectively, similar to our peptide system, and the authors concluded that the peptide adopted a β-sheet structure with unique π–π interactions, based on the results of FT–IR measurements [39]. Thus, the present CD measurements suggest that RU003 transformed from a random coil to a β-sheet conformation after a lag period. We previously reported time-dependent CD spectra of RU003 TDs alone and found that RU003 TDs quickly adopted stable b-sheet structures, probably due to increased hydrophobicity and extended amide bonds for hydrogen bonds in the literature [33].

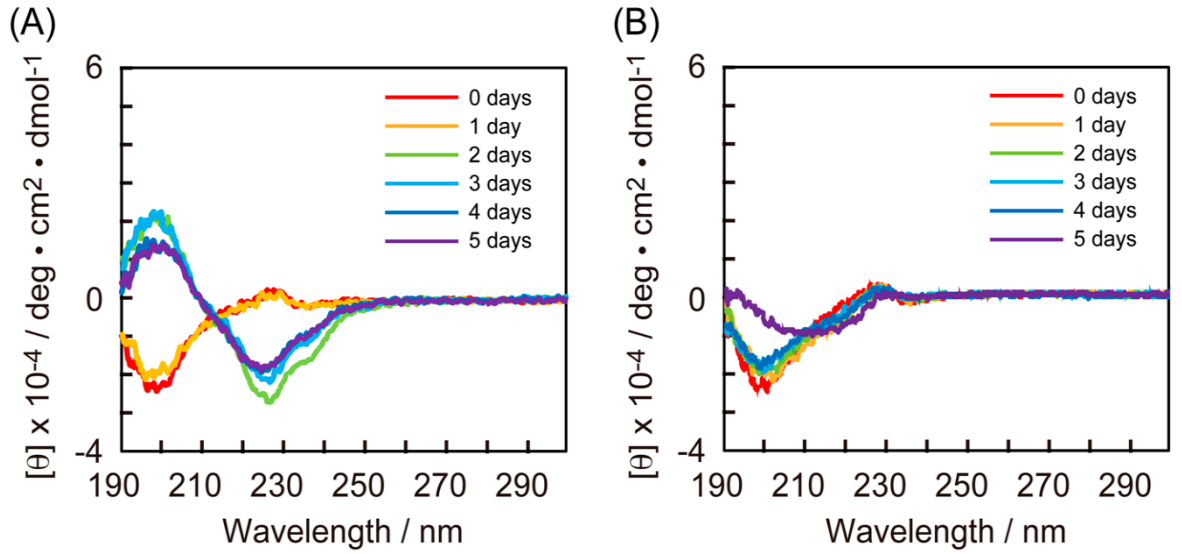

Figure 2. Typical circular dichroism (CD) spectra of RU003 in the (**A**) absence and (**B**) presence of Ape5-TD (conditions: [RU003] = 100 μM and [Ape5-TD] = 10 μM in water at 40 °C). The *y*-axis indicates the mean residue ellipticity. Incubation period "0 day" means "5 min after the reaction started".

3.3. CD Measurements of the Mixtures of RU003 Monomer and Ape-TD

Figure 2B shows that the CD spectra of the mixture of RU003 (100 μM) and Ape5-TD (10 μM) remained essentially unchanged (random coil conformation) for 4 days, with a strong negative peak at 200 nm, followed by a weak structural transition (a CD spectrum corresponding to mixed random coil and β-sheet conformation) at day-5. These findings surprisingly indicated that Ape5-TD,

a tandem-homodimer of RU003, inhibited the random-to-β structural transition of RU003, with a lag time of at least 4 days at a substoichiometric ratio.

We also preliminarily attempted to monitor the peptide self-assembling processes by thioflavin T (ThT) assay, which is the common technique for monitoring Ab fibrillation (Figure S13). However, the fluorescence intensity of ThT mixed with the RU003 sample solution taken from the reaction mixture ([RU003] = 100 mM) at day-3 was much smaller than that for Ape5-TD alone ([Ape5-TD] = 10 mM), even at lower peptide concentration than RU003, and ThT fluorescence intensity mixed with Ape5-TD showed a nonmonotonic change as a function of elapsed time (Figure S13B). We, therefore, focused on the changes in mean residue ellipticity at 225 nm in the CD spectra of mixtures of RU003 and RU003 TDs to assess the potency of RU003 TDs to inhibit the random-to-β structural transition of RU003.

3.4. CD Measurements of the Mixtures of RU003 Monomer and RU003 TDs

We obtained typical time-dependent CD spectra of mixtures of RU003 and the tandem-homodimers Abu4-TD (Figure S14), Ape5-TD (Figure S15), Ahx6-TD (Figure S16), Ahp7-TD (Figure S17), and Aoc8-TD (Figure S18), then summarized the changes in mean residue ellipticity at 225 nm as a function of time (Figure 3). Coincubation of RU003 (100 μM) and Abu4-TD (5.0 μM) significantly inhibited the random-to-β structural transition of RU003, and the lag time for the transition increased with increasing Abu4-TD concentration. In particular, 20 μM Abu4-TD prevented the random-to-β structural transition of RU003 until day-5 (Figure S14 and Figure 3A). Figure S15 and Figure 3B show that the addition of Ape5-TD (5.0 and 10 μM) completely prevented the random-to-β structural transition of RU003 until day-4, and only weak structural transition was observed at day-5. Increasing the Ape5-TD concentration to 20 μM also resulted in significant inhibition of the structural transition by day-4, followed by partial β-sheet structure formation at day-5. Figure S16 and Figure 3C show that the Ahx6-TD (5.0 μM) sample prevented the random-to-β structural transition of RU003 until day-2, then the amount of β-sheet conformation increased gradually until day-5. The Ahx6-TD (10 and 20 μM) samples showed a mixture of random coil and early β-sheet conformations at day-0, remained unchanged until day-2, then underwent a structural transition. Ahp7-TD (5.0, 10, and 20 μM) retained the random coil structure at day-2, with Ahp7-TD (10 μM) showing better inhibitory activity than 5.0 and 20 μM Ahp7-TD (Figure S17 and Figure 3D). The Aoc8-TD (5.0 and 20 μM) samples showed the same time-dependent profiles as RU003 alone, indicating an inability to inhibit the random-to-β structural transition of RU003 (Figure S18 and Figure 3E), although 10 μM Aoc8-TD slightly inhibited the structural transition of RU003 by day-2. In all cases, the day-0 CD spectra of samples containing 10 and 20 μM RU003-TD showed a slightly red-shifted negative peak (from 200 to 205 nm), together with a shoulder or weak negative peak around 220 nm, probably due to the early β-sheet structures of RU003 TDs [33].

3.5. Comparison of the Half-life Periods for the Random Peptide Structures

We quantitatively compared the inhibitory activities of RU003 TDs to the random-to-β structural transition of RU003 and revealed the effects of the linker chain length by calculating the half-life periods ($t\frac{1}{2}$) for the random structures (elapsed time to acquire a mean residue ellipticity of -1.0×10^{-4} deg cm^2 dmol^{-1}) to transition to a β structure, using the data in Figure 3. The RU003 monomer showed a $t\frac{1}{2}$ value of ca. one and a half days. The addition of Ape5-TD (5.0, 10, and 20 μM) to RU003 afforded the greatest delay effects (which were differences between the $t\frac{1}{2}$ value in the absence and presence of RU003 TDs on the structural transition) of 3 days or longer, followed by Abu4-TD (20 μM) and Ahx6-TD (5.0 μM), with the delay effects of ca. 2 days. The other peptides gave delay effects of 1 day or less. These results suggest that (i) a tandem-homodimer connected with a short linker, such as Abu4, requires high TD concentration to exhibit significant inhibitory activity on the random-to-β structural transition of RU003; (ii) a tandem-homodimer connected with a long linker, such as Ahx6, needs a low TD concentration but shows moderate inhibitory activity; (iii) tandem-homodimers connected with longer linkers, such as Ahp7 and Aoc8, showed insignificant inhibitory activity even at elevated

concentrations of RU003 TDs, probably due to preorganization of the TDs, resulting in reduced effective TD concentrations toward fibrillation inhibition. Consequently, a tandem-homodimer connected with a six-atom-length alkanoic acid (Ape5) is the best molecular design for preventing the random-to-β structural transition of RU003.

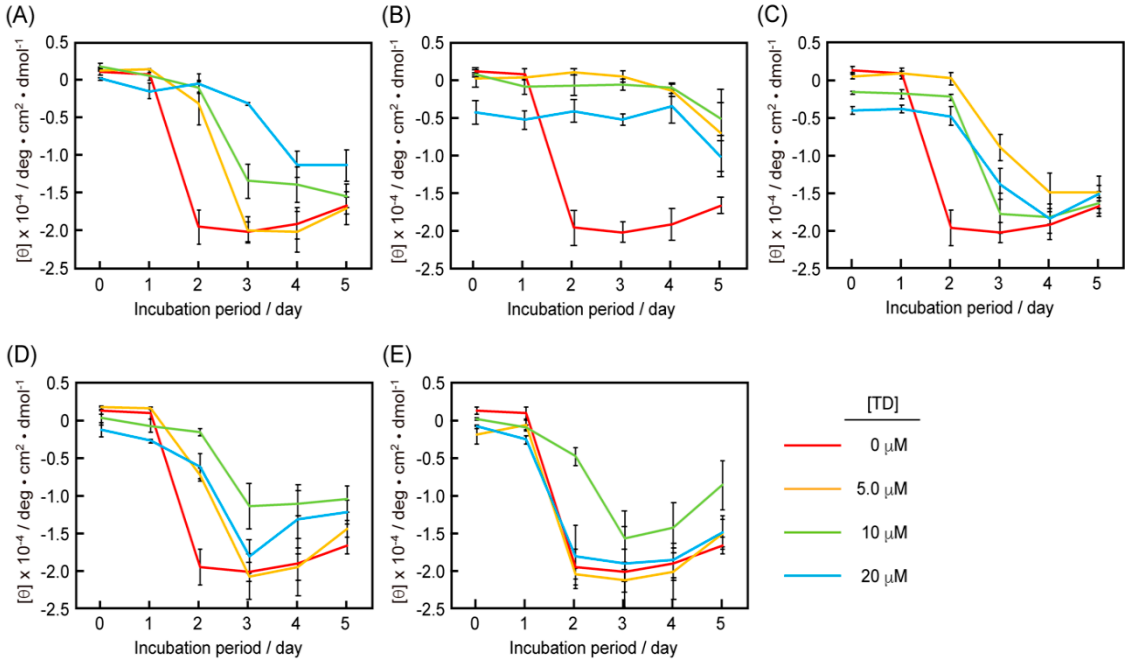

Figure 3. The mean residue ellipticity at 225 nm of the CD spectra of RU003 in the absence and presence of the RU003 tandem-homodimers (**A**) Abu4-TD, (**B**) Ape5-TD, (**C**) Ahx6-TD, (**D**) Ahp7-TD, and (**E**) Aoc8-TD as a function of incubation period (conditions: [RU003] = 100 μM and [TD] = 0, 5.0, 10, and 20 μM in water at 40 °C, mean ± SD, n = 3). These data were derived from Figures S1–S5.

3.6. TEM and AFM Measurements of the Peptide Self-Assemblies

Given these time-dependent structural transitions of the peptides, we observed mixtures of RU003 (100 μM) and RU003 TDs (10 μM), matured for 5 days, using transmission electron microscopy (TEM) to understand the morphology of the stable self-assembled structures. The TEM images in Figure S19 show twisted ribbon-like fibrous structures ca. 10 nm in width for all samples. However, only the TEM image of the sample coincubated with Ape5-TD showed a significant number of disordered large aggregates, with diameters of 100 nm or larger, comprising many spherical peptide self-assemblies ca. 30 nm in width, together with regularly arranged, twisted nanoribbons (Figure S19C). We conducted atomic force microscopic (AFM) analyses of the same samples studied by CD and TEM (but on a silicon wafer) to investigate the disordered large aggregates (Figure 4). Figure 4A shows an AFM image of RU003 self-assemblies (100 μM) prepared by 5-day incubation. We observed many regular fibrous nanostructures ca. 4 nm in height, similar to the molecular length of an extended RU003, adopting a β-sheet conformation, and ca. 8 nm in height, double the molecular length of RU003 and likely corresponding to the thickness of overlapping twisted nanoribbons and/or flat nanoribbons. An AFM image of a mixture of RU003 (100 μM) and Ape5-TD (10 μM), matured for 5 days, revealed disordered, somewhat globular structures that were several tens of nanometers in height. The AFM and TEM results were in good agreement. We, therefore, concluded that the RU003 TD with an Ape5 linker inhibited the random-to-β structural transition, caused disordered large peptide aggregates, and formed aggregates that were stable for 5 days.

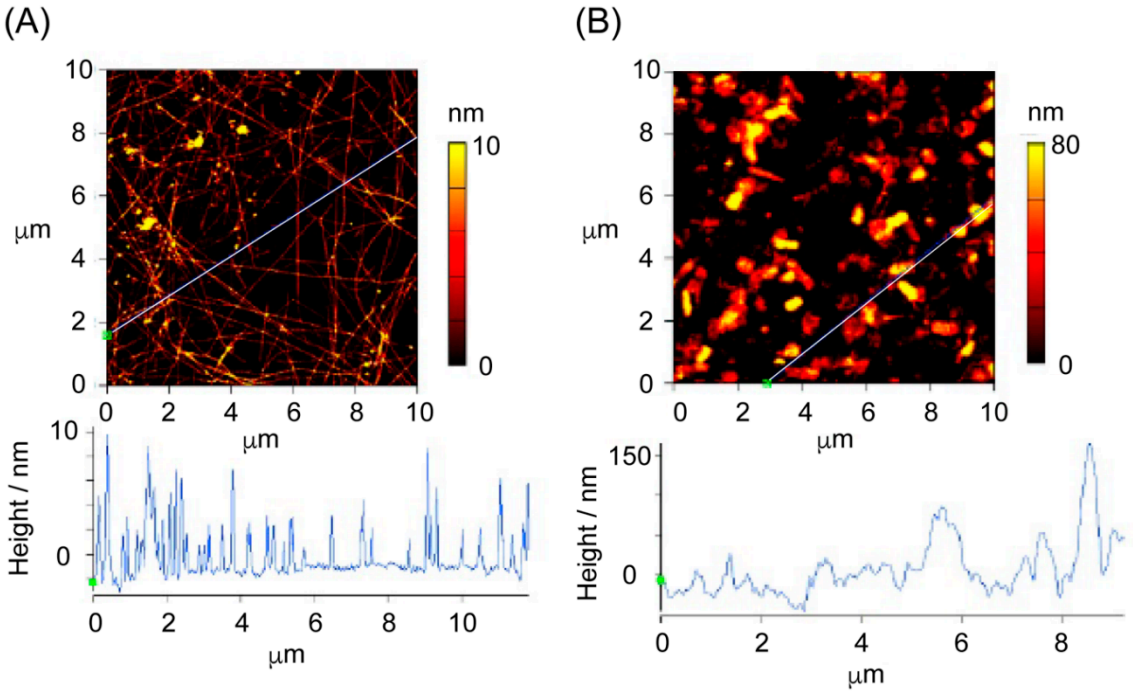

Figure 4. Atomic force microscopy (AFM) images of RU003 in the (**A**) absence and (**B**) presence of Ape5-TD incubated in water at 40 °C for 5 days (conditions: [RU003] = 100 μM and [TD] = 10 μM). Top and bottom panels indicate tapping mode AFM images and section analysis of the samples, respectively.

3.7. Proteolytic Stability of the Peptide Self-Assemblies

Disordered large peptide aggregates were obtained by mixing RU003 and Ape5-TD in a ratio of 10/1 (mol/mol). These aggregates were different from fibrous structures with a regular β-sheet conformation. Interestingly, Nilsson et al. reported that hydrogel networks composed of different alignment modes of amphiphilic peptides showed various proteolytic stabilities and rheological strengths [31]. If the disordered structures observed in the current study were proteolytically labile relative to regularly arranged fibrous structures, the globular aggregates would be digested by intrinsic enzymes, preventing the accumulation of peptide self-assemblies. We, therefore, examined the proteolytic stabilities of the self-assembled fibrous structures comprising RU003 (100 μM) and the disordered aggregates coassembled by RU003 (100 μM) and Ape5-TD (10 μM) in the presence of trypsin and α-chymotrypsin. Figure 5A shows HPLC profiles of RU003-based fibrous structures in the absence (-) and presence (+) of trypsin. Proteolysis of the self-assembled fibrous structures of RU003 resulted in a decrease in the intensity of peak *a* (corresponding to RU003) and an increase in the intensity for peak *c* (corresponding to peptide fragments), indicating that ca. 14.5% of RU003 was digested by trypsin during the reaction period. The disordered aggregates of RU003 and Ape5-TD were more labile to proteolysis than the RU003 self-assembled fibrous structures, with ca. 27.6% of RU003 being digested by trypsin (Figure 5B). On the other hand, Figure 5C,D show HPLC profiles for the α-chymotryptic digestion of RU003 self-assembled fibrous structures and disordered aggregates of RU003 and Ape5-TD, respectively, and indicate that ca. 26.4% and 25.6% of RU003 were degraded by α-chymotrypsin, respectively. These proteolytic degradation results suggest that disordered aggregates comprising RU003 and Ape5-TD are more trypsin-labile than regularly arranged fibrous RU003 self-assemblies. However, both self-assembled structures showed similar proteolytic susceptibility to α-chymotrypsin, likely due to the positively charged Lys side chains being near the surface of disordered aggregates during coassembly but inside the regularly assembled RU003 fibrous structures stabilized by intermolecular interactions, including cation–π interactions.

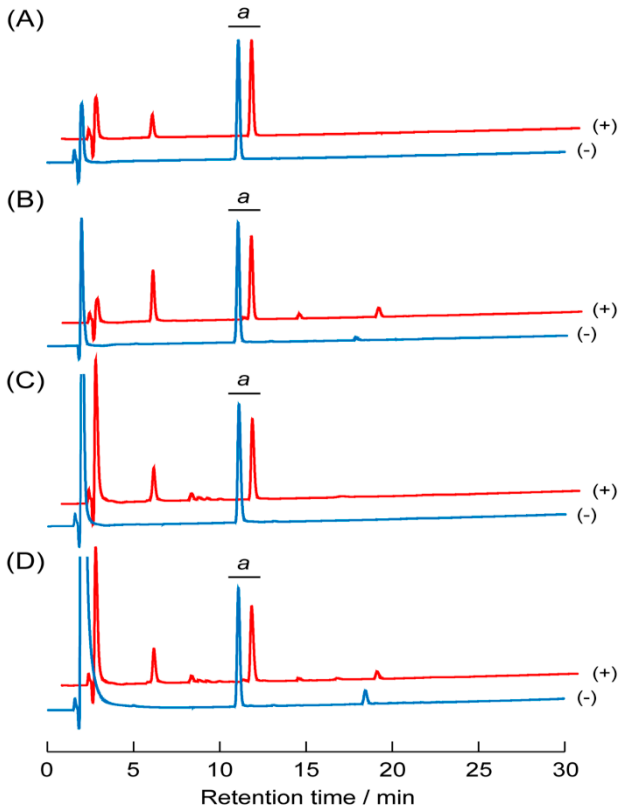

Figure 5. HPLC profiles of the reaction mixtures of (**A**,**C**) RU003 (100 μM) and (**B**,**D**) RU003 (100 μM) and Ape5-TD (10 μM), matured for 5 days, followed by proteolytic degradation with (**A**,**B**) trypsin from bovine pancreas (RU003/trypsin = 490/1, *w*/*w*) and (**C**,**D**) chymotrypsin from bovine pancreas (RU003/chymotrypsin = 1/1, *w*/*w*). Samples were incubated at 40 °C for 1 h and analyzed by reversed-phase HPLC. The symbols "+" and "-" in parentheses indicate HPLC profiles "with" and "without" proteases, respectively. "*a*" denotes the peaks for RU003.

3.8. Possible Inhibitory Process

In this study, we mixed RU003 and RU003 TDs at substoichiometric ratios and analyzed changes in the secondary structures of the mixtures with time by CD spectroscopic measurements. The CD spectra of the mixtures at day-0 showed slightly red-shifted negative peaks around 200 nm, together with a shoulder or weak negative peak around 220 nm, likely indicating the coexistence of an RU003 monomer forming a random coil structure and a small amount of RU003 TD oligomers forming β-sheet structures at the early stage of self-assembly (Figure 2 and Figure S14–S18. The RU003 TDs, especially Ape5-TD oligomers with strong hydrophobic site(s), could accommodate the hydrophobic Nal and Ile side chains of RU003 monomers, causing the RU003 monomers to adopt twisted conformations, potentially reducing regular intermolecular contacts, stabilizing and expanding the β-sheet structure, and inducing irregular accumulation of RU003 monomers, leading to disordered large aggregates composed of RU003 and RU003 tandem-homodimers (Figure 4and Figure S19). Tryptic digestion experiments showed that the disordered aggregates of RU003 and Ape5-TD were more labile to proteolysis than the fibrous structure composed of RU006 in a regular β-sheet conformation. In contrast, there was no significant difference in the susceptibility of the two structures to chymotryptic digestion (Figure 5), indicating that the twisted conformation of RU003 monomers flipped the Lys side chains outside the aggregate structure, preventing the stabilization of regular β-sheet structures via cation–π interactions and allowing easy access of trypsin. Hydrophobic Nal side chains remained embedded deep inside the aggregates. The CD and proteolytic digestion experiments were in good agreement with each other.

We previously analyzed the hydrophobicities of self-assembled fibrous structures of RU003 and RU003 tandem-homodimers, matured for 7 days using the 1-anilinonaphthalene sulfonic acid (ANS)

binding assay, and found that (i) Abu4-TD exhibited slightly greater ANS affinity than RU003, (ii) Ape5-TD, Ahx6-TD, and Ahp7-TD showed much stronger ANS affinity, and (iii) Aoc8-TD showed affinity equal to that of RU003 [33]. Therefore, we concluded that Ape5, Ahx6, and Ahp7 adopted a bent (hairpin) conformation with hydrophobic site(s) large enough to accommodate an ANS molecule but not large enough for the shortest RU003, and the longest Aoc8-TD forced an extended conformation [33]. From these results, Abu4-TD, which has relatively weak hydrophobic site(s), had to be present at high concentration to prevent the random-to-β structural transition of RU003. Aoc8-TD, which has the longest alkyl linker, did not significantly inhibit RU003 β-sheet formation due to difficulty in accessing the RU003 monomers in the hydrophobic interior of Aoc8-TD oligomer/protofilament structures. Furthermore, the longer linkers of Ahx6-TD and Ahp7-TD, compared with Ape5, increased the strain of the peptide bent conformation and reduced the binding affinity of the RU003 monomers. Consequently, the Ape5-TD linker had an excellent balance of length and hydrophobicity, suitable for accommodating RU003 monomers. It is noteworthy that the present tandem-homodimer system requires 5.0–10 mol% of the target peptide and forms proteolytically labile aggregates. Although this study used a model system to examine inhibitory activity towards the random-to-β structural transition of the target peptide, the present tandem-homodimerization system could be advantageous for the molecular design of modulators for amyloid fibrillogenesis.

4. Conclusions

The presented tandem-homodimerization method was effective in preventing the random-to-β structural transition of the original monomer at a substoichiometric ratio, and the subsequent disordered peptide aggregates were more readily proteolytically digested than fibrous structures composed of RU003 adopting a β-sheet conformation. Of the five RU003 TDs containing amino alkanoic acid linkers (i.e., Abu4, Ape5, Ahx6, Ahp7, and Aoc8), Ape5-TD most effectively prevented the random-to-β structural transition of RU003 for at least 5 days by generating disordered aggregates with reducing tryptic stability. The inhibitory effects of the linkers in the RU003 TDs on structural transitions probably resulted from their bent conformations and hydrophobicity, which were appropriate for accommodating and twisting RU003 monomers, causing irregular arrangements of the peptides. This series of RU003 and RU003 tandem-homodimers is a model system for Aβ-associated diseases, and the orientation of the peptides in the nanostructures is still unclear. Further investigations are required to, for example, optimize linkers for tandem-homodimers by using naturally occurring amino acid sequences or other functional groups and reveal the precise orientation of the peptides in the nanostructures, making the tandem-homodimerization method generally applicable to the rational design of a new class of fibrillogenesis modulators.

Supplementary Materials: The following are available online at http://www.mdpi.com/2227-9717/8/11/1421/s1. Figure S1: Analytical HPLC profile for RU003; Figure S2: MALDI–TOF–MS for RU003; Figure S3: Analytical HPLC profile for Abu4-TD; Figure S4: MALDI–TOF–MS for Abu4-TD; Figure S5: Analytical HPLC profile for Ape5-TD; Figure S6: MALDI–TOF–MS for Ape5-TD; Figure S7: Analytical HPLC profile for Ahx6-TD; Figure S8: MALDI–TOF–MS for Ahx6-TD; Figure S9: Analytical HPLC profile for Ahp7-TD; Figure S10: MALDI–TOF–MS for Ahp7-TD; Figure S11: Analytical HPLC profile for Aoc8-TD; Figure S12: MALDI–TOF–MS for Aoc8-TD; Figure S13: Thioflavin T assay for RU003 and Ape5-TD alone; Figure S14: Time-dependent CD spectra of the mixtures of RU003 and Abu4-TD; Figure S15: Time-dependent CD spectra of the mixtures of RU003 and Ape5-TD; Figure S16: Time-dependent CD spectra of the mixtures of RU003 and Ahx6-TD; Figure S17: Time-dependent CD spectra of the mixtures of RU003 and Ahp7-TD; Figure S18: Time-dependent CD spectra of the mixtures of RU003 and Aoc8-TD; Figure S19: TEM images of the mixtures of RU003 and RU003 tandem-homodimers.

Author Contributions: Conceptualization, K.-y.T.; data curation, T.I. (Tomomi Iori), H.F., Y.N., and Y.M.; funding acquisition, K.-y.T.; investigation, K.-y.T., T.I. (Tomomi Iori), H.F., Y.N., Y.M., and T.I. (Takahito Imai); methodology, K.-y.T.; project administration, K.-y.T.; supervision, K.-y.T.; writing—original draft, K.-y.T.; writing—review and editing, K.-y.T. All authors have read and agreed to the published version of the manuscript.

Funding: This study was supported in part by the 2020 Ryukoku University Joint Research Center for Science and Technology Fund and JSPS KAKENHI Grant Numbers JP16K05854 and JP20K05713.

Acknowledgments: The authors acknowledge Kei Takayama, Tomohiro Kamada, Tomotaka Hieno, Mizuki Nakakita, and Takeru Okamoto for preliminary data curation for this research project. Electron microscopy images were obtained at the Ryukoku University Electron Microscope Laboratory.

Conflicts of Interest: The authors declare no conflict of interest.

References

1. Selkoe, D.J. Folding proteins in fatal ways. *Nat. Cell Biol.* **2003**, *426*, 900–904. [CrossRef] [PubMed]
2. Lu, J.X.; Qiang, W.; Yau, W.M.; Schwieters, C.D.; Meredith, S.C.; Tycko, R. Molecular structure of β-amyloid fibrils in Alzheimer's disease brain tissue. *Cell* **2013**, *154*, 1257–1268. [CrossRef] [PubMed]
3. Lansbury, P.T.; Lashuel, H.A. A century-old debate on protein aggregation and neurodegeneration enters the clinic. *Nat. Cell Biol.* **2006**, *443*, 774–779. [CrossRef] [PubMed]
4. Haass, C.; Selkoe, D.J. Soluble protein oligomers in neurodegeneration: Lessons from the Alzheimer's disease and type II diabetes. *Chem. Soc. Rev.* **2012**, *8*, 101–112.
5. Hamley, I.W. The Amyloid Beta Peptide: A Chemist's Perspective. Role in Alzheimer's and Fibrillization. *Chem. Rev.* **2012**, *112*, 5147–5192. [CrossRef] [PubMed]
6. Hamley, I.W.; Castelletto, V. Self-Assembly of Peptide Bioconjugates: Selected Recent Research Highlights. *Bioconjugate Chem.* **2016**, *28*, 731–739. [CrossRef]
7. Powers, E.T.; Powers, D.L. Mechanisms of Protein Fibril Formation: Nucleated Polymerization with Competing Off-Pathway Aggregation. *Biophys. J.* **2007**, *94*, 379–391. [CrossRef]
8. Findeis, M.A. Approaches to discovery and characterization of inhibitors of amyloid β-peptide polymerization. *Biochim. Biophys. Acta* **2000**, *1502*, 76–84. [CrossRef]
9. Taylor, M.; Moore, S.; Mayers, J.; Parkin, E.; Beeg, M.; Canovi, M.; Gobbi, M.; Mann, D.M.A.; Allsop, D. Development of a proteplytically stable retro-inverso peptide inhibitor of β-amyloid oligomerization as a potential novel treatment for Alzheimer's disease. *Biochemistry* **2010**, *49*, 3261–3272. [CrossRef]
10. Castelletto, V.; Ryumin, P.; Cramer, R.; Hamley, I.W.; Taylor, M.; Allsop, D.; Reza, M.; Ruokolainen, J.; Arnold, T.; Hermida-Merino, D.; et al. Self-Assembly and Anti-Amyloid Cytotoxicity Activity of Amyloid beta Peptide Derivatives. *Sci. Rep.* **2017**, *7*, 43637. [CrossRef]
11. Han, X.; Park, J.; Wu, W.; Malagon, A.; Wang, L.; Vargas, E.; Wikramanayake, A.; Houk, K.N.; Leblanc, R.M. A resorcinrene for inhibition of Aβ fibrillation. *Chem. Sci.* **2017**, *8*, 2003–2009. [CrossRef]
12. Jia, L.; Zhao, W.; Sang, J.; Wang, W.; Wei, W.; Wang, Y.; Zhao, F.; Lu, F.; Liu, F. Inhibitory Effect of a Flavonoid Dihydromyricetin against Aβ40 Amyloidogenesis and Its Associated Cytotoxicity. *ACS Chem. Neurosci.* **2019**, *10*, 4696–4703. [CrossRef]
13. Sagnou, M.; Mavroidi, B.; Kaminari, A.; Boukos, N.; Pelecanou, M. Novel isatin thiosemicarbazone derivatives as potent inhibitors of β-amyloid peptide aggregation and toxicity. *ACS Chem. Neurosci.* **2020**, *11*, 266–2276. [CrossRef]
14. Kumar, S.; Hamilton, A.D. α-Helix Mimetics as Modulators of Aβ Self-Assembly. *J. Am. Chem. Soc.* **2017**, *139*, 5744–5755. [CrossRef] [PubMed]
15. Luo, J.; Yu, C.-H.; Yu, H.; Borstnar, R.; Kamerlin, S.C.; Gräslund, A.; Abrahams, J.P.; Wärmländer, S.K. Cellular polyaminespromote amyloid-beta (Aβ) peptide fibrillation and modulate the aggregation pathways. *ACS Chem. Neurosci.* **2013**, *4*, 454–462. [CrossRef] [PubMed]
16. Liu, H.; Ojha, B.; Morris, C.; Jiang, M.; Wojcikiewicz, E.P.; Rao, P.P.N.; Du, D. Positively Charged Chitosan and N-Trimethyl Chitosan Inhibit Aβ40 Fibrillogenesis. *Biomacromolecules* **2015**, *16*, 2363–2373. [CrossRef] [PubMed]
17. Bucciantini, M.; Giannoni, E.; Chiti, F.; Baroni, F.; Formigli, L.; Zurdo, J.; Taddei, N.; Ramponi, G.; Dobson, C.M.; Stefani, M. Inherent toxicity of aggregates implies a common mechanism for protein misfolding diseases. *Nat. Cell Biol.* **2002**, *416*, 507–511. [CrossRef]
18. Kirkitadze, M.D.; Bitan, G.; Teplow, D.B. Paradigm shifts in Alzheimer's disease and other neurodegenerative disorders: The emerging role of oligomeric assemblies. *J. Neurosci. Res.* **2002**, *69*, 567–577. [CrossRef]
19. Goedert, M.; Spillantini, M.G. A Century of Alzheimer's Disease. *Science* **2006**, *314*, 777–781. [CrossRef]
20. Haass, C.; Selkoe, D.J. Soluble protein oligomers in neurodegeneration: Lessons from the Alzheimer's amyloid β-peptide. *Nat. Rev. Mol. Cell Biol.* **2007**, *8*, 101–112. [CrossRef]

21. Taneja, V.; Verma, M.; Vats, A. Toxic species in amyloid disorders: Oligomers or mature fibrils. *Ann. Indian Acad. Neurol.* **2015**, *18*, 138–145. [CrossRef]
22. Mroczko, B.; Groblewska, M.; Litman-Zawadska, A.; Kornhuber, J.; Lewczuk, P. Amyloid β oligomers (AβOs) in Alzheimer's disease. *J. Neural Transm.* **2018**, *125*, 177–191. [CrossRef] [PubMed]
23. Bitan, G.; kirkitadze, M.D.; Lomakin, A.; Vollers, S.S.; Benedek, G.B.; Teplow, D.B. Amyloid β-protein (Aβ) assembly: Aβ40 and Aβ42 oligomerize through distinct pathways. *Proc. Natl. Acad. Sci. USA* **2003**, *100*, 330–336. [CrossRef] [PubMed]
24. Urbanc, B.; Cruz, L.; Yun, S.; Buldyrev, S.V.; Bitan, G.; Teplow, D.B.; Stanley, H.E. In silico study, of amyloid β-protein folding and oligomerization. *Proc. Natl. Acad. Sci. USA* **2004**, *101*, 17345–17350. [CrossRef]
25. Murakami, K. Conformation-specific antibodies to target amyloid β oligomers and their application to immunotherapy for Alzheimer's disease. *Biosci. Biotechnol. Biochem.* **2014**, *78*, 1293–1305. [CrossRef] [PubMed]
26. Li, H.; Rahimi, F.; Bitan, G. Modulation of amyloid β-protein assembly by homologous C-terminal fragments as a strategy for inhibiting Aβ toxicity. *ACS Chem. Neurosci.* **2016**, *7*, 845–856. [CrossRef]
27. Deike, S.; Rothemund, S.; Voigt, B.; Samantray, S.; Strodel, B.; Binder, W.H. β-Turn mimetis synthetic peptides as amyloid-β aggregation inhibitors. *Bioorg. Chem.* **2020**, *101*, 104013. [CrossRef]
28. Mustafi, S.M.; Garai, K.; Crick, S.L.; Baban, B.; Frieden, C. Substoichiometric inhibition of Aβ1-40 aggregation by a tandem Aβ40-1-Gly8-Aβ1-40 peptide. *Biochim. Biophys. Res. Commun.* **2010**, *397*, 509–512. [CrossRef]
29. Klein, A.N.; Ziehm, T.; Tusche, M.; Buitenhuis, J.; Bartnik, D.; Böddrich, A.; Wiglenda, T.; Wanker, E.E.; Funke, S.A.; Brener, O.; et al. Optimization of the All-D Peptide D3 for Aβ Oligomer Elimination. *PLoS ONE* **2016**, *11*, e0153035. [CrossRef]
30. Riek, R.; Güntert, P.; Döbeli, H.; Wipf, B.; Wüthrich, K. NMR studies in aqueous solution fail to identify significant conformational differences between the monomeric forms of two Alzheimer peptides with widely different plaque-competence, Aβ(1–40)ox and Aβ(1–42)ox. *JBIC J. Biol. Inorg. Chem.* **2001**, *268*, 5930–5936. [CrossRef]
31. Swanekamp, R.J.; Weich, J.J.; Nilsson, B.L. Proteolytic stability of amphipathic peptide hydrogels composed of self-assembled pleated β-sheet or coassembled rippled β-sheet fibrils. *Chem. Commun.* **2014**, *50*, 10133–10136. [CrossRef]
32. Tomizaki, K.-Y.; Kubo, S.; Ahn, S.-A.; Satake, M.; Imai, T. Biomimetic Alignment of Zinc Oxide Nanoparticles along a Peptide Nanofiber. *Langmuir* **2012**, *28*, 13459–13466. [CrossRef]
33. Tomizaki, K.-Y.; Tanaka, A.; Shimada, H.; Nishizawa, K.; Wada, T.; Imai, T. The alkyl linkers in tandem-homodimers of a β-sheet-forming nonapeptide affect the self-assembled nanostructures. *Bioorg. Med. Chem. Lett.* **2016**, *26*, 2659–2662. [CrossRef]
34. Diaferia, C.; Gianolio, E.; Sibillano, T.; Mercurio, F.A.; Leone, M.; Giannini, C.; Balasco, N.; Vitagliano, L.; Morelli, G.; Accardo, A. Cross-beta nanostructures based on dinaphthylalanine Gd-conjugates loaded with doxorubicin. *Sci. Rep.* **2017**, *7*, 1–14. [CrossRef] [PubMed]
35. Sadqi, M.; Lapidus, L.J.; Muñoz, V. How fast is protein hydrophobic collapse? *Proc. Natl. Acad. Sci. USA* **2003**, *100*, 12117–12122. [CrossRef]
36. Chan, W.C.; White, P.D. *Fmoc Solid Phase Peptide Synthesis: A Practical Approach*; Oxford University Press: New York, NY, USA, 2000; pp. 41–76.
37. Manavalan, P.; Jr, W.C.J. Sensitivity of circular dichroism to protein tertiary structure class. *Nat. Cell Biol.* **1983**, *305*, 831–832. [CrossRef]
38. Bowerman, C.J.; Liyanage, W.; Federation, A.J.; Nilsson, B.L. Tuning β-Sheet Peptide Self-Assembly and Hydrogelation Behavior by Modification of Sequence Hydrophobicity and Aromaticity. *Biomacromolecules* **2011**, *12*, 2735–2745. [CrossRef]
39. Lee, N.R.; Bowerman, C.J.; Nilsson, B.L. Effects of Varied Sequence Pattern on the Self-Assembly of Amphipathic Peptides. *Biomacromolecules* **2013**, *14*, 3267–3277. [CrossRef] [PubMed]